

Single-photon optical bistability in a small nonlinear cavityIgor E. Protsenko * and Alexander V. Uskov *P.N. Lebedev Physical Institute of the RAS, Moscow 119991, Russia*

(Received 12 May 2023; accepted 7 August 2023; published 23 August 2023)

We theoretically investigated the bistability in a small Fabry-Perot interferometer (FPI) with the optical wavelength size cavity, the nonlinear Kerr medium, and only a few photons, on average, excited by the external quantum field. Analytical expressions for the stationary mean photon number, the bistability domain, the field, and the photon number fluctuation spectra are obtained. Multiple stationary states of the FPI cavity field with different spectra are possible at realistic conditions, for example, in the FPI with the photonic crystal cavity and the semiconductor-doped glass nonlinear medium.

DOI: [10.1103/PhysRevA.108.023724](https://doi.org/10.1103/PhysRevA.108.023724)**I. INTRODUCTION**

Recent technological progress has led to a considerable reduction of the optical integrated circuit element size [1,2] in photonic quantum technologies (PQT) [3]. An essential element of PQT is a miniature Fabry-Perot interferometer (FPI) [4–6] to be part of a variety of devices, such as the optical delay lines [7], the wavelength-division multiplexers [8], laser cavities [9], and so on. The bistable miniature FPI is considered an essential element for PQT and is necessary for ultra-low photonic signal processing [10,11]. FPI with a nonlinear medium has optical bistability [12–14] and operates as an optical transistor [15], where noiseless amplification is possible [15,16].

A small FPI, with a cavity of the size of the optical wavelength, is appropriate for PQT. When the nonlinear Kerr medium is in the FPI cavity, the cavity refractive index and the FPI mode frequency depend on the number of the cavity photons, leading to *dispersive* optical bistability at certain conditions [12–14,17]. In particular, a nonzero detuning between the FPI mode and the input field frequencies is necessary for bistability [14]. The detuning reduces the number of photons in the FPI cavity. Thus, one expects a small number of photons in a small FPI with the detuning, as we will see below. So it is essential to investigate whether a bistability is possible with only a few, one or even less than one photon, on average, in the FPI cavity. Such investigation is complicated because the photon fluctuations cannot be neglected or considered perturbations of a small number of photons. The purpose of this paper is to contribute to such an investigation.

Here we analyze, by the analytical approach, the bistability in the small FPI with the nonlinear Kerr medium, excited by the field where the quantum fluctuations are significant and not a perturbation. The linearized theory previously analyzed optical bistability in the FPI with the field quantum fluctuations considered perturbations [18]. Meanwhile, the exact quantum steady-state equation of [18], found with

the help of P-representation, did not exhibit bistability or hysteresis.

Section II describes a simplified model of the nonlinear FPI, (i.e., the FPI with a nonlinear Kerr medium inside) shown in Fig. 1, with only one semitransparent mirror. We write equations of motion for such a model. Section III presents analytical formulas for the field, and the photon number fluctuation spectra of the mode of the FPI introduced in Sec. II. The derivation of formulas of Sec. III is given in the Appendix. Section III generalizes results for a simple FPI in Fig. 1 to the FPI with two semitransparent mirrors shown in Fig. 2. Section IV describes the bistability conditions for the nonlinear FPI, excited by the external quantum field and shows the example of the FPI field spectra at the bistability. Section V estimates the values of parameters necessary for the optical bistability in the small FPI with a few photons in the cavity. We discuss the results in the discussion Sec. VI and finalize the paper in the conclusion in Sec. VII.

II. MODEL AND EQUATIONS OF MOTION

To simplify the analysis, we consider, in the beginning, the FPI with only one semitransparent and one perfectly reflecting mirror, is shown in Fig. 1. Then we generalize the approach to the FPI with two semitransparent mirrors shown in Fig. 2.

The cavity of the FPI is filled with the Kerr medium whose refractive index depends on the cavity field intensity. The mode of the FPI cavity is excited by the quantum input field taken from a laser or a light-emitting diode (LED). The input field Bose operator is $\hat{a}_{\text{in}}e^{-i\omega_{\text{in}}t}$; \hat{a}_{in} is the field amplitude operator, and the input field spectrum is centered on the optical carrier frequency ω_{in} . The input field enters the FPI through the semitransparent mirror with the transmission rate κ .

We suppose that the FPI cavity length is $\lambda/2$, where λ is the input field wavelength and assume that the main FPI cavity mode is excited; ω_{in} is close to the frequency ω_0 of the center of the excited FPI mode spectrum. We neglect the excitation of the other FPI modes.

The output field with the amplitude Bose operator \hat{a}_{out} leaves the FPI through the semitransparent mirror. The

*protsenk@gmail.com

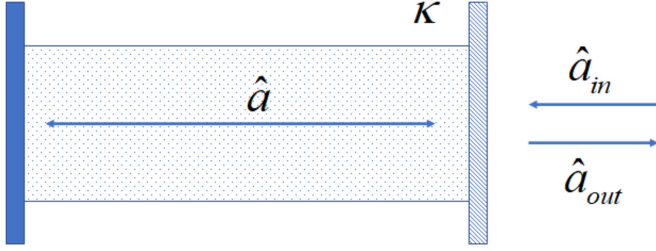


FIG. 1. Scheme of the nonlinear FPI with the semitransparent mirror on the right and the perfectly reflected mirror on the left. Notations are explained in the text.

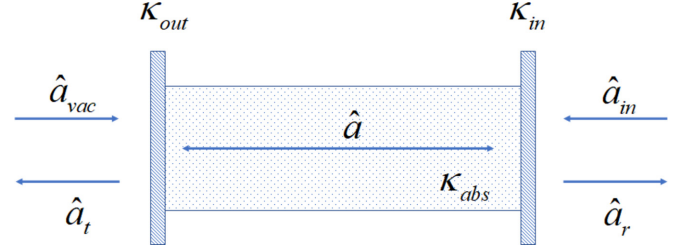


FIG. 2. The scheme of the nonlinear FPI with two semitransparent mirrors. \hat{a}_{vac} is the vacuum field coming through the output mirror. The rest of the notations are explained in the text.

amplitude Bose operator of the excited FPI mode is \hat{a} . The input and the output field mean powers are $p_{in} = \langle \hat{a}_{in}^+ \hat{a}_{in} \rangle$, and $p_{out} = \langle \hat{a}_{out}^+ \hat{a}_{out} \rangle$, respectively. We denote quantum-mechanical averaging as $\langle \dots \rangle$, the mean values (and the c-number coefficients) by letters without hats (as a), and operators by letters with hats (as \hat{a}).

The Hamiltonian of the FPI shown in Fig. 1 written in the interaction picture, the rotating wave approximation, and with the normal ordering of Bose operators is

$$H = \hbar \delta_0 \hat{a}^+ \hat{a} - \frac{\hbar \delta_1}{2} \hat{a}^+ \hat{a}^+ \hat{a} \hat{a} + \hat{\Gamma}, \quad (1)$$

where the detuning $\delta_0 = \omega_0 - \omega_{in} \ll \omega_0, \omega_{in}$; δ_1 is the nonlinearity coefficient of the Kerr medium, the multiplier $-1/2$ in $-\hbar \delta_1/2$ is introduced for convenience; $\hat{\Gamma}$ describes the input field coming to the FPI and the field leaving the FPI through the semitransparent mirror. Note that $\delta_1 \sim \tilde{n}_2/V$, where \tilde{n}_2 is the Kerr medium nonlinear coefficient used in the literature [19] and V is the FPI cavity mode volume. A small V , of the size about the optical wavelength, provides a large δ_1 , enough for the bistability with only a few photons in the FPI cavity, as discussed in Sec. VI.

Hamiltonian (1) leads to the Heisenberg equation of motion for \hat{a}

$$\dot{\hat{a}} = -(i\delta_0 + \kappa)\hat{a} + i\delta_1 \hat{n} \hat{a} + \sqrt{2\kappa} \hat{a}_{in}, \quad (2)$$

where $\hat{n} = \hat{a}^+ \hat{a}$ is the photon number operator. The terms $-\kappa \hat{a}$ and $\sqrt{2\kappa} \hat{a}_{in}$ describe the cavity field decay and the external field coming through the semitransparent mirror. According to the input-output theory [20,21] these terms are added to Eq. (2).

If the FPI is excited by the coherent classical field, and quantum fluctuations of the FPI field are neglected, then the operators \hat{a} and \hat{a}_{in} in Eq. (2) must be replaced by c-number variables a and a_{in} ; the photon number operator \hat{n} is replaced by $|a|^2$, so Eq. (2) turns into the classical equation has multiple stationary solutions [12–14,17].

The quantum equation (2) can be solved, in principle, by the perturbation procedure: We separate in \hat{n} the mean photon

number n and the photon number fluctuations $\delta \hat{n}$; insert $\hat{n} = n + \delta \hat{n}$ into Eq. (2), neglect by $\delta \hat{n}$ and obtain

$$\dot{\hat{a}} = -(i\delta_0 + \kappa)\hat{a} + i\delta_1 n \hat{a} + \sqrt{2\kappa} \hat{a}_{in}. \quad (3)$$

Equation (3) is linear in operators and can be solved by the operator Fourier transform. The mean photon number n can be found from the stationary solution of Eq. (3) by the procedure similar to the one in [22–24] used for the laser equations.

Equation (2) can be approximated by Eq. (3) if the photon number fluctuations are small relative to n . It is not true at $n \leq 1$ when the photon number fluctuations are not small and cannot be neglected. The following sections show how to modify Eq. (3) when the photon number fluctuations are not small.

III. FLUCTUATION SPECTRA

We represent operators in Eq. (2) by Fourier expansions

$$\hat{A}(t) = (2\pi)^{-1} \int_{-\infty}^{\infty} \hat{A}(\omega) e^{-i\omega t} d\omega, \quad (4)$$

where \hat{A} means \hat{a} , \hat{a}_{in} , or $\hat{n}\hat{a}$; obtain the algebraic relation for the Fourier component operator $\hat{a}(\omega)$, and find a formal solution

$$\hat{a}(\omega) = \frac{i\delta_1 (\hat{n}\hat{a})_{\omega} + \sqrt{2\kappa} \hat{a}_{in}(\omega)}{i(\delta_0 - \omega) + \kappa}. \quad (5)$$

Here $(\hat{n}\hat{a})_{\omega}$ is the Fourier component of the operator product $\hat{n}\hat{a}$. Note that we use the multiplier $e^{-i\omega t}$ in Fourier expansions. In particular,

$$\hat{A}^+(t) = (2\pi)^{-1} \int_{-\infty}^{\infty} (\hat{A}^+)_{\omega} e^{-i\omega t} d\omega. \quad (6)$$

It follows from Eqs. (4) and (6) that the Fourier-component operator $(\hat{A}^+)_{\omega} = [\hat{A}(-\omega)]^+ \equiv \hat{A}^+(-\omega)$.

The stationary field spectrum $n(\omega)$ satisfies the relation $\langle (\hat{a}^+)_{\omega} \hat{a}(\omega') \rangle = n(\omega) \delta(\omega + \omega')$. Using Eq. (5), we find

$$n(\omega) = \frac{\delta_1^2 \langle (\hat{a}^+ \hat{n})_{-\omega} (\hat{n} \hat{a})_{\omega} \rangle + i\delta_1 \sqrt{2\kappa} [\langle \hat{a}_{in}^+(\omega) (\hat{n} \hat{a})_{\omega} \rangle - \langle (\hat{a}^+ \hat{n})_{-\omega} \hat{a}_{in}(\omega) \rangle] + 2\kappa p_{in}(\omega)}{(\delta_0 - \omega)^2 + \kappa^2}, \quad (7)$$

where $p_{\text{in}}(\omega) = \langle \hat{a}_{\text{in}}^+(\omega) \hat{a}_{\text{in}}(\omega) \rangle$ is the input field power spectrum. To find $n(\omega)$ we must calculate $\langle (\hat{a}^+ \hat{n})_{-\omega} (\hat{n} \hat{a})_{\omega} \rangle$ and $\langle \hat{a}_{\text{in}}^+(\omega) (\hat{n} \hat{a})_{\omega} \rangle$. It is found in the Appendix that

$$\langle \hat{a}_{\text{in}}^+(\omega) (\hat{n} \hat{a})_{\omega} \rangle = \frac{2n\sqrt{2\kappa} p_{\text{in}}(\omega)}{i(\delta_n - \omega) + \kappa}, \quad (8)$$

where δ_n is a nonlinear detuning

$$\delta_n = \delta_0 - 2\delta_1 n. \quad (9)$$

The energy conservation law for the FPI in Fig. 1 requires $p_{\text{in}}(\omega) = p_{\text{out}}(\omega)$, where $p_{\text{out}}(\omega) = \langle \hat{a}_{\text{out}}^+(\omega) \hat{a}_{\text{out}}(\omega) \rangle$ is the output field power spectrum. It follows from the energy conservation law that

$$\langle (\hat{a}^+ \hat{n})_{-\omega} (\hat{n} \hat{a})_{\omega} \rangle = \frac{8\kappa n^2 p_{\text{in}}(\omega)}{(\delta_n - \omega)^2 + \kappa^2}, \quad (10)$$

as shown in the Appendix. Substituting the results (8) and (10) and $\langle (\hat{a}^+ \hat{n})_{-\omega} \hat{a}_{\text{in}}(\omega) \rangle = \langle \hat{a}_{\text{in}}^+(\omega) (\hat{n} \hat{a})_{\omega} \rangle^*$ into Eq. (7) we find the FPI cavity mode spectrum

$$n(\omega) = \frac{2\kappa p_{\text{in}}(\omega)}{(\delta_n - \omega)^2 + \kappa^2}. \quad (11)$$

In a similar way, we obtain the spectrum $(n+1)_{\omega}$ of the antinormal ordered operator product $\hat{a} \hat{a}^+$. $(n+1)_{\omega}$ is given by Eq. (11) with the replacement of $p_{\text{in}}(\omega)$ by $p_{\text{in}}(\omega) + 1$. Thus, we find a ‘‘commutator spectrum’’ $[\hat{a}, \hat{a}^+]_{\omega} = (n+1)_{\omega} - n(\omega) \equiv c(\omega)$

$$c(\omega) = \frac{2\kappa}{(\delta_n - \omega)^2 + \kappa^2}, \quad (12)$$

$(2\pi)^{-1} \int_{-\infty}^{\infty} [\hat{a}, \hat{a}^+]_{\omega} d\omega = 1$ as it must be for the cavity-mode Bose operators [20,21].

Formulas (11) and (12) and the formula

$$\begin{aligned} \delta^2 n(\omega) &= \frac{1}{2\pi} \int_{-\infty}^{\infty} n(\omega + \omega') n(\omega') d\omega' \\ &+ \frac{1}{4\pi} \int_{-\infty}^{\infty} [n(\omega' + \omega) + n(\omega' - \omega)] c(\omega') d\omega' \end{aligned} \quad (13)$$

derived in [25] let us find the stationary field $n(\omega)$ and the photon number fluctuation $\delta^2 n(\omega)$ spectra of the FPI cavity mode excited by the external quantum field.

One can see that the results (11) and (12) follow from an effective Hamiltonian

$$H_{\text{eff}} = \hbar(\delta_0 - 2\delta_1 n) \hat{a}^+ \hat{a} + \hat{\Gamma} \quad (14)$$

quadratic in operators \hat{a} and \hat{a}^+ . Taking into account $\langle \hat{a}^+ \hat{a}^+ \hat{a} \hat{a} \rangle = 2n^2$, we note that the mean $2\hbar\delta_1 n \langle \hat{a}^+ \hat{a} \rangle = 2\hbar\delta_1 n^2$ of the nonlinear term in the effective Hamiltonian (14) is *two times larger* than the mean $(\hbar\delta_1/2) \langle \hat{a}^+ \hat{a}^+ \hat{a} \hat{a} \rangle = \hbar\delta_1 n^2$ of the nonlinear term in the exact Hamiltonian (1).

The analysis in the Appendix, leading to results (11) and (12), takes into account the photon number fluctuations, neglected in the term $i\delta_1 n \hat{a}$ in the approximate Eq. (3). The replacement $\delta_1 \rightarrow 2\delta_1$ in Eq. (3) (equivalent to the replacement of the Hamiltonian H by H_{eff}) leads to the same results as the ones found in the Appendix and, therefore, enough for taking into account the photon number fluctuations related

to the nonlinear term in Hamiltonian (1), at least for the calculations of n , $n(\omega)$, and $\delta^2 n(\omega)$ in the stationary case.

We use the effective Hamiltonian (14) to analyze of the FPI with two semi-transparent mirrors in the following subsection.

FPI with two semitransparent mirrors

Now we consider the FPI with two semitransparent mirrors, the nonlinear medium, and the linear absorption inside the cavity. We denote κ_{in} , (κ_{out}) the transmission rate of the input (output) FPI mirrors; κ_{abs} is the rate of the linear absorption in the FPI cavity. The field with the amplitude operator \hat{a}_r is reflected from the input mirror and the field with the operator \hat{a}_t is transmitted through the FPI, as shown in Fig. 2. The effective Hamiltonian for the FPI in Fig. 2 is the same as H_{eff} given by Eq. (14) with only the dissipative term $\hat{\Gamma}$ being different.

There are three dissipative channels in the FPI in Fig. 2: Two semitransparent mirrors and the linear absorption in the cavity. We derive Heisenberg equations of motion for \hat{a} from the effective Hamiltonian (14), adding dissipative terms for each channel to the equation of motion following the input-output theory [20,21]. We solve the equation of motion the same way as Eq. (2), obtaining the FPI cavity field spectrum

$$n(\omega) = \frac{2\kappa_{\text{in}} p_{\text{in}}(\omega)}{(\delta_n - \omega)^2 + \kappa_{\text{cav}}^2} \quad (15)$$

and the cavity field commutator spectrum [see Eq. (12)]

$$c(\omega) = \frac{2\kappa_{\text{cav}}}{(\delta_n - \omega)^2 + \kappa_{\text{cav}}^2}. \quad (16)$$

Here

$$\kappa_{\text{cav}} = \kappa_{\text{in}} + \kappa_{\text{out}} + \kappa_{\text{abs}} \quad (17)$$

is the FPI cavity mode decay rate for all decay channels. Formulas (15) and (16), together with formula (13), let us calculate the stationary mean photon number, the field, and the photon number fluctuation spectra of the mode of the FPI shown in Fig. 2.

IV. OPTICAL BISTABILITY WITH A SMALL NUMBER OF PHOTONS

A. Stationary mean values

We rewrite the photon number and the commutator spectra (15) and (16) as

$$n(\omega) = (\kappa_{\text{in}}/\kappa_{\text{cav}}) p_{\text{in}}(\omega) L(\omega + \delta_n, \kappa_{\text{cav}}). \quad (18)$$

and

$$c(\omega) = L(\omega + \delta_n, \kappa_{\text{cav}}). \quad (19)$$

Here and below

$$L(\omega, \kappa) = 2\kappa/(\omega^2 + \kappa^2) \quad (20)$$

is a normalized Lorentz function, $(2\pi)^{-1} \int_{-\infty}^{\infty} L(\omega, \kappa) d\omega = 1$. We take the spectrum $p_{\text{in}}(\omega)$ of the input field, with the half-width κ_s

$$p_{\text{in}}(\omega) = p_{\text{in}} L(\omega, \kappa_s), \quad (21)$$

where p_{in} is the FPI input power in photons per second.

Using the identity $(2\pi)^{-1} \int_{-\infty}^{\infty} L(\omega + \delta, \kappa_1)L(\omega, \kappa_2) = L(\delta, \kappa_1 + \kappa_2)$ and relations (18) and (21) we calculate the mean photon number in the FPI mode

$$n = \frac{1}{2\pi} \int_{-\infty}^{\infty} n(\omega)d\omega = p_{\text{eff}}L(\delta_n, \kappa_{\text{eff}}), \quad (22)$$

where

$$p_{\text{eff}} = (\kappa_{\text{in}}/\kappa_{\text{cav}})p_{\text{in}}, \quad \kappa_{\text{eff}} = \kappa_s + \kappa_{\text{cav}}, \quad (23)$$

the nonlinear detuning δ_n is determined by Eq. (9).

The power of the field transmitted through the FPI is $p_{\text{out}} = 2\kappa_{\text{out}}n$ or

$$p_{\text{out}} = 2\kappa_{\text{out}}p_{\text{eff}}L(\delta_n, \kappa_{\text{eff}}). \quad (24)$$

The result for the semi-classical case [12,13] is recovered from Eq. (24) at $\kappa_s = 0$, so $\kappa_{\text{eff}} = \kappa_{\text{cav}}$; the multiplier 2 must be removed from the expression (9) for the nonlinear detuning δ_n .

B. Bistability conditions

We find the bistability conditions from Eq. (22) the way similar to the semi-classical optical bistability theory [12] and the catastrophe theory [13,26].

We introduce normalized parameters

$$Y = 2p_{\text{eff}}/\kappa_{\text{eff}}, \quad \Delta_0 = \delta_0/\kappa_{\text{eff}}, \quad \Delta_1 = 2\delta_1/\kappa_{\text{eff}}, \quad (25)$$

considering Y as a function of n and rewrite Eq. (22) as

$$Y = Y(n) \equiv n[1 + (\Delta_0 - n\Delta_1)^2]. \quad (26)$$

Equation (26) is well-known in the semi-classical theory of dispersive optical bistability in the cavity [12]. Parameters (25), however, are different from ones in the semi-classical theory where $2\delta_1$ and $\kappa_{\text{eff}} = \kappa_{\text{cav}} + \kappa_s$ must be replaced, respectively, by δ_1 and κ_{cav} .

Equation (26) is a cubic equation for n with one, two, or three real roots depending on the values of Y and $\Delta_{0,1}$ [27]. We plot $Y(n)$ in Fig. 3 and see, that Eq. (26) has two roots, when

$$\partial Y(n)/\partial n = 0 \quad (27)$$

is satisfied together with Eq. (26). Solving the set of equations (26) and (27), respectively, to n and Y we find the roots of Eq. (26)

$$n_{\pm} = (2\Delta_0 \pm \sqrt{\Delta_0^2 - 3})/3\Delta_1, \quad (28)$$

at $Y_{\pm} = 2p_{\pm}/\kappa_{\text{eff}}$, where

$$p_{\pm} = \kappa_{\text{eff}}n_{\pm}[1 + (\Delta_0 - n_{\pm}\Delta_1)^2]/2, \quad (29)$$

Equations (28) and (29) define a surface, separating regions with one and three solutions of Eq. (26) in the parameter space. Three solutions of Eq. (26) exist at $p_- < p < p_+$, otherwise there is only one solution, as shown in Fig. 3.

According to Eq. (28) n_{\pm} is real and, therefore, the parameter region with three solutions exists, if $\Delta_0^2 \geq 3$, which means that

$$|\delta_0| > \delta_{\text{min}} = \sqrt{3}\kappa_{\text{eff}}. \quad (30)$$

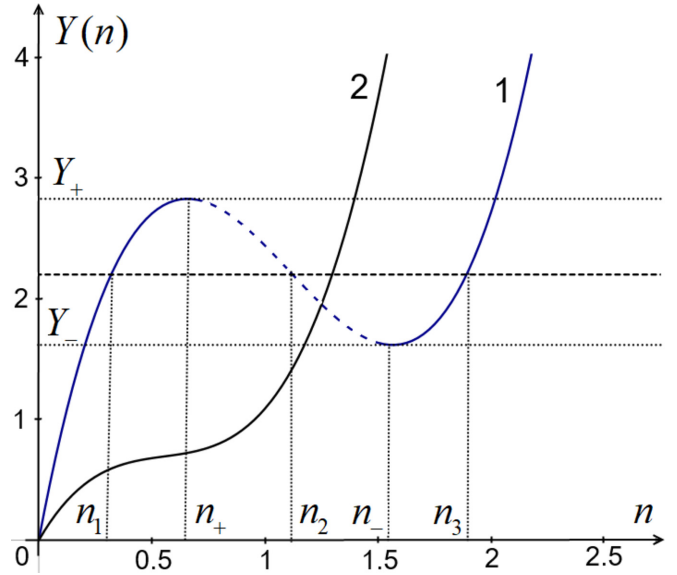


FIG. 3. The normalized input field power Y , given by Eq. (26), as a function of the mean photon number n . When the condition (30) is satisfied, there are three stationary n : $n_1 < n_2 < n_3$ for some Y , $Y_- < Y < Y_+$, shown by the horizontal line crossing curve 1. The dashed part of curve 1 corresponds to the unstable stationary solution as n_2 . Equation (26) has two stationary solutions when $Y = Y_{\pm}$. One of the solutions at $Y = Y_+$ is n_+ , the solution at $Y = Y_-$ is n_- ; n_{\pm} is given by Eq. (28). There is only one stationary n for any Y , when condition (30) is not true, as for curve 2.

So the absolute value of the detuning δ_0 must be sufficiently large to have multiple stationary solutions.

Following the semi-classical analysis and applying the Heisenberg correspondence principle [28], we suppose that the solution n_2 from three solutions $n_1 < n_2 < n_3$ of Eq. (26) (see Fig. 3) is unstable and two other solutions $n_{1,3}$ are stable relatively small deviations. So Eqs. (28) and (29) determine the borders of the FPI *bistability* region in the parameter space.

Taking n_{\pm} positive we see from Eqs. (28) and (25) that δ_0 and δ_1 must have the same signs for bistability. Physically, it means a positive feedback between the mean number of photons n and the nonlinear detuning δ_n . Note the minus sign in Eq. (9) for δ_n : While n grows, the detuning δ_n decreases, providing, in turn, the increase of n at $\delta_0 > 0$.

If we slowly decrease p_{eff} from some $p_{\text{eff}} > p_+$ or increase p_{eff} from $p_{\text{eff}} < p_-$ and cross the bistability region $p_+ < p < p_-$, the transition from one stationary FPI state to another state happens at $p_{\text{eff}} = p_{\pm}$.

Figure 4 shows the bistability regions inside the area restricted by $p_{\pm}(\delta_0)$ solid curves for the quantum FPI with $\delta_1/\kappa_{\text{cav}} = 1.8$ and $\kappa_s/\kappa_{\text{cav}} = 1$. The dashed curves in Fig. 4 restrict the bistability region for the classical FPI with $\delta_1/\kappa_{\text{cav}} = 1.8$, $\kappa_s = 0$, and δ_1 replaced by $\delta_1/2$ in Eq. (29). The bistability region for the quantum FPI is smaller. It begins at the larger detuning than the bistability region for the classical FPI. Figure 5 shows examples of the stationary $n(\delta_0)$ for the quantum and the classical FPI at some p_{eff} values with or without the bistability in the FPI. Similar curves are presented, for example, in [29] for the classical nonlinear oscillator. We

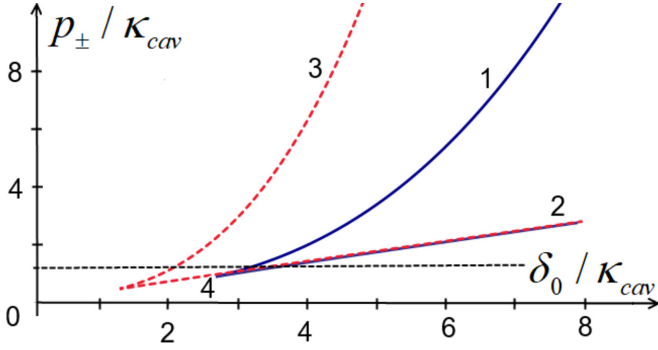


FIG. 4. The bistability region for the quantum FPI is between the solid curves $p_{\pm}(\delta_0)$ (curves 1 and 2; $p_+ > p_-$); there is only one stationary n otherwise. Curves are plotted for $\delta_1/\kappa_{cav} = 1.8$, $\kappa_s/\kappa_{cav} = 1$. The dashed curves 3 and 4 restrict the bistability region for the semi-classical FPI. The dashed horizontal line marks the value $p_{eff}/\kappa_{cav} = 1.3$ taken for $n(\delta_0)$ curves 3 and 6 in Fig. 5.

see from Figs. 4 and 5 that the bistability regions and the stationary n are substantially different for the quantum and the classical FPI.

Figure 6 shows the input field spectrum given by Eq. (21) (the dashed curve 1) and the output field spectra $p_{out}(\omega) = 2\kappa_{out}n(\omega)$ for parameters belonging to the bistability region; $\kappa_{in} = \kappa_{out}$, $\kappa_{abs} = 0$, $\delta_0/\kappa_{cav} = 4.4$, $\delta_1/\kappa_{cav} = 1.8$, $\kappa_s/\kappa_{cav} = 1$, and $p_{eff}/\kappa_{cav} = 1.3$. The field has two stationary states in the FPI: With $n = 1.3$ and $n = 0.4$; spectra 2 and 3, respectively, shown in Fig. 6, correspond to these states. Each stationary state has a specific field and photon number fluctuation spectra. The integration of $\delta^2n(\omega)$ [see Eq. (13)] over frequencies demonstrates the photon number variance

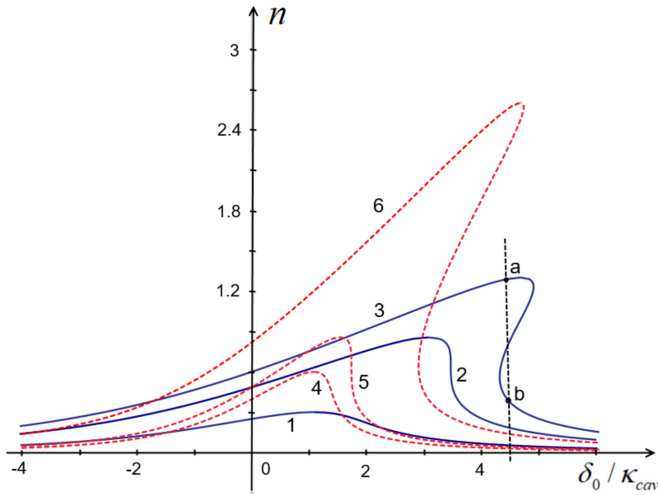


FIG. 5. Stationary $n(\delta_0)$ of the quantum FPI shown by the solid curves 1,2,3 for $p_{eff}/\kappa_{cav} = 0.3, 0.855$ and 1.3 ; correspondingly, $\delta_1/\kappa_{cav} = 1.8$, $\kappa_s/\kappa_{cav} = 1$; and for the semi-classical FPI shown by the dashed curves 4, 5, and 6 for $p_{eff}/\kappa_{cav} = 0.3, 0.428$, and 1.3 . There is no bistability in curves 1 and 4 for a small p_{eff} ; curves 2 and 5 correspond to the very beginning of the bistability region in Fig. 4 at $p_+ = p_-$; the bistability is for curves 3 and 6. The vertical dashed line marks $\delta_0/\kappa_{eff} = 4.4$; points a and b correspond to two coexisting stationary solutions with spectra shown in Fig. 6.

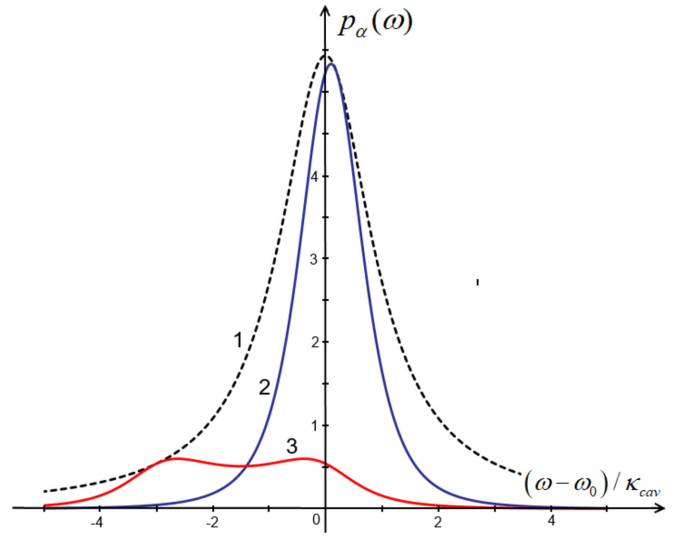


FIG. 6. The input field spectrum, $\alpha = in$ (the dashed curve 1) and the output field spectra $\alpha = out$ (the solid curves 2 and 3) of two stationary states of the FPI coexisting at the bistability when $\delta_0/\kappa_{cav} = 4.4$. Two stationary $n = 1.3$ and 0.4 correspond to the spectra curves 2 and 3 and points a and b , respectively, on the $n(\delta_0)$ curve 3 in Fig. 5.

$\delta^2n = n(n + 1)$ for both stationary states (with a different n for each state) [25].

V. PARAMETERS FOR THE BISTABILITY WITH A FEW PHOTONS

The results found above let us estimate when bistability is possible in a small FPI with the nonlinear Kerr medium and a few photons inside.

According to the authors of [19], the field-dependent refractive index n_r of the Kerr medium is

$$n_r = n_0 + \tilde{n}_2 I, \tag{31}$$

where I is the intensity of the field, and \tilde{n}_2 is a nonlinearity coefficient in the refractive index, n_0 is the field-independent part of n_r . For certainty, we consider $\tilde{n}_2 > 0$ as it is in many semiconductors, such as Si or GaAs [19]. As usual, we suppose $\tilde{n}_2 I \ll n_0$.

We consider a Fabri-Perot cavity, shown in Fig. 2, with Kerr medium with the nonlinear refractive index n_r given by Eq. (31). The field of the intensity I is in the FPI main cavity mode. We express $n_r(I)$ in the mean number of photons n in the FPI cavity. We take $I = (n_0 c / 8\pi) |E|^2$ [30], where c is the speed of light in a vacuum, and E is the field amplitude. In the quantum case, $|E|^2$ is replaced by $\langle \hat{E}^+ \hat{E} \rangle$, where the field amplitude operator $\hat{E} = \sqrt{4\pi \hbar \omega_0 / V} \hat{a}$, \hat{a} is a Bose operator [31], V is the cavity-mode volume, ω_0 is the carrier frequency of the FPI mode. So we rewrite Eq. (31) in $n = \langle \hat{a}^+ \hat{a} \rangle$

$$n_r = n_0 + n_2 n, \tag{32}$$

where

$$n_2 = \tilde{n}_2 n_0 c \hbar \omega_0 / 2V. \tag{33}$$

We will estimate how large the nonlinear coefficient \tilde{n}_2 of the refractive index (31) must be for the bistability when the mean number of photons in the FPI cavity $n = 1$.

The resonant frequency ω_m of the cavity mode is [30]

$$\omega_m = \frac{\pi cm}{(n_0 + n_2 n)L} \approx \omega_0(1 - n_2 n/n_0), \quad (34)$$

where $\omega_0 = \pi cm/n_0 L$, L is the length of the cavity, the integer $m = 1$ for the FPI main cavity mode, and $n_2 n \ll n_0$. We see $2\delta_1 = \omega_0 n_2/n_0 \sim \tilde{n}_2/V$ from Eqs. (33), (34), and (9).

According to conditions (30), the bistability appears when the external field frequency is detuned from the cavity mode frequency at least on $\delta_0 = \sqrt{3}\kappa_{\text{eff}}$ where κ_{eff} is the sum of all linewidths and decay rates given by Eqs. (23) and (17). We express $2\kappa_{\text{eff}} = \omega_0/Q$, where Q is an effective quality factor of the main FPI cavity mode. Expressing δ_1 and κ_{eff} in Eq. (30) through n_2 , Q , and other parameters, we find that the bistability is possible when $2n_2 n/\sqrt{3}n_0 \geq 1/Q$ or, taking n_2 from Eq. (33), when

$$\tilde{n}_2 c(\hbar\omega_0/\sqrt{3}V)nQ \geq 1. \quad (35)$$

Condition (35) with $n = 1$ estimates the minimum value $\min \tilde{n}_2$ of \tilde{n}_2 necessary for the bistability with only a few photons inside the FPI cavity. It must be

$$\tilde{n}_2 > \min \tilde{n}_2 = \sqrt{3}V/(c\hbar\omega_0 Q). \quad (36)$$

We take the frequency ω_0 corresponding to the wavelength $\lambda_0 = 1.55 \mu\text{m}$; the volume of the main FPI cavity mode $V = (\lambda_0/2n_0)^3$, the linear refractive index $n_0 = 3.3$ as in [32]; $Q = 10^3$. The quality factor $Q \sim 10^3/10^4$ is achievable, for example, in the photonic crystal microcavities [33]. For such parameters, it must be $\tilde{n}_2 > 10^{-6} \text{ cm}^2/\text{kWt}$ for the bistability with only a few photons in the FPI cavity. Such nonlinearity is achievable, for example, in semiconductor-doped glasses with a nonlinear response time $\sim 10^{-10}/10^{-11} \text{ s}$ [19].

VI. DISCUSSION

We find the bistability in the stationary states of the FPI with a small number of photons in the cavity when the FPI is excited by the quantum field and the quantum fluctuations of the field are not small.

As a hypothesis, we assume that the upper and lower branches of the stationary $n(\delta_0)$ curve in Fig. 4 correspond to the stationary states stable to small deviations from the stationary state, as it is in the classical bistability [26]. Such a stability hypothesis must be rigorously proved for the quantum case elsewhere in the future.

Each stationary state of the FPI has its own fluctuations and spectra, as, for example, the field spectra shown in Fig. 6. This is the difference between the classical FPI excited by the monochromatic field when only the stationary cavity or the output fields (with no fluctuations) can be determined.

The bistability conditions for the quantum case are different from the ones in the semi-classical case [12,13]. The linewidth of the input field is added to the total relaxation rate of the FPI cavity mode, as in Eq. (23), and the effective nonlinear coefficient $2\delta_1$ in the nonlinear detuning (9) is two times

larger than the nonlinear coefficient δ_1 in the semi-classical case.

The transition from one another stationary state occurs at $n = n_{\pm}$ given by Eq. (28) when the stationary FPI states are on the borders of the bistability region in Fig. 5. We do not analyze the dynamics of such transitions. Transitions between multiple classical stationary states were studied, for example, in [34].

We show that the stationary mean photon number and the low-order correlations: The field, and the photon number fluctuation spectra can be found from the effective Hamiltonian (14). It is shown in the Appendix that these results are a good approximation of the exact results corresponding to the exact Hamiltonian (1) in the stationary case. We did not analyze the nonstationary dynamics (including small deviations from the stationary states) and the higher-order correlations. It will be done in the future. The low-order stationary correlations found here are enough for practical purposes in many cases [35].

Relations (A2), necessary for our calculations, are held in the stationary case. With relations (A2), the cluster expansion approximation lets us replace the mean of the four-order operator product in the integral in Eq. (A1) by the sum (A3) of the binary operator products. We use the energy conservation law to determine the frequency domain's fourth-order correlations; see Eq. (A8) and comments in the Appendix.

Specific field and the photon number fluctuation spectra inside and outside the cavity of the linear FPI are found in [25]. The spectra of the nonlinear FPI can be obtained by replacing the detuning δ_0 in [25] with the nonlinear detuning $\delta_0 - 2\delta_1 n$.

We estimate that multiple stationary solutions are possible in a small FPI cavity, of the size of the order of the optical wavelength, with a few photons and the nonlinear Kerr medium as, for example, semiconductor-doped glass.

VII. CONCLUSION

We predict multiple stationary states in the theoretical model of the small Fabry-Perot interferometer (FPI) with a nonlinear Kerr medium and a few photons in the mode excited by an external quantum field. Such multiple solutions are necessary for optical bistability. The stationary mean photon number, the bistability conditions, the field, and the photon number fluctuation spectra are found analytically. Estimations show that the multiple solutions appear at realistic conditions, for example, in the photonic crystal FPI cavity of the size of the optical wavelength with a semiconductor-doped glass nonlinear medium. The results are helpful for the investigation, construction, and applications of small nonlinear elements with FPI, as optical transistors, in the photonic integrated circuits operating with quantum fields. Our treatment of the FPI with a nonlinear medium presents an example of solving the quantum nonlinear oscillator equations analytically.

We hope the present results stimulate the experimental studies of optical bistability in a small FPI with the nonlinear Kerr medium and the quantum field.

APPENDIX: CALCULATIONS OF CORRELATIONS

Here we find $\langle \hat{a}_{\text{in}}^+(\omega) (\hat{n}\hat{a})_{\omega} \rangle$ appears in Eq. (7). The operator product Fourier component is a convolution

$$(\hat{n}\hat{a})_{\omega} = (2\pi)^{-1/2} \int_{-\infty}^{\infty} \hat{n}(\omega - \omega_1) \hat{a}(\omega_1) d\omega_1,$$

$$\hat{n}(\omega - \omega_1) = (2\pi)^{-1/2} \int_{-\infty}^{\infty} \hat{a}^+(\omega_2 + \omega_1 - \omega) \hat{a}(\omega_2) d\omega_2.$$

Therefore,

$$(\hat{n}\hat{a})_{\omega} = (2\pi)^{-1/2} \int_{-\infty}^{\infty} d\omega_1 d\omega_2 \hat{a}^+(\omega_2 + \omega_1 - \omega) \hat{a}(\omega_2) \hat{a}(\omega_1)$$

and

$$\begin{aligned} \langle \hat{a}_{\text{in}}^+(\omega) (\hat{n}\hat{a})_{\omega} \rangle &= \frac{1}{2\pi} \int_{-\infty}^{\infty} d\omega_1 \int_{-\infty}^{\infty} d\omega_2 \\ &\times \langle \hat{a}_{\text{in}}^+(\omega) \hat{a}^+(\omega_2 + \omega_1 - \omega) \hat{a}(\omega_2) \hat{a}(\omega_1) \rangle. \end{aligned} \quad (\text{A1})$$

We simplify the integral (A1) using relations

$$\begin{aligned} \langle \hat{a}^+(\omega') \hat{a}(\omega) \rangle &= n(\omega) \delta(\omega' - \omega), \\ \langle \hat{a}(\omega') \hat{a}^+(\omega) \rangle &= (n+1)_{\omega} \delta(\omega' - \omega), \end{aligned} \quad (\text{A2})$$

which hold in the stationary case. In Eq. (A2) $n(\omega)$ is the field spectrum; we denote $(n+1)_{\omega}$ the spectrum for the antinormally ordered operator product $\hat{a}(\omega') \hat{a}^+(\omega)$.

It follows from relations (A2) that $\langle \hat{a}^+(\omega') \hat{a}(\omega) \rangle = 0$ and $\hat{a}^+(\omega')$ commute with $\hat{a}(\omega)$ if $\omega \neq \omega'$. Therefore, $\hat{a}^+(\omega')$ does not correlate with $\hat{a}(\omega)$ at $\omega \neq \omega'$ at the stationary case and we replace the mean value in the integral (A1) by

$$\begin{aligned} &\langle \hat{a}_{\text{in}}^+(\omega) \hat{a}(\omega_2) \rangle \langle \hat{a}^+(\omega_2 + \omega_1 - \omega) \hat{a}(\omega_1) \rangle \\ &+ \langle \hat{a}_{\text{in}}^+(\omega) \hat{a}(\omega_1) \rangle \langle \hat{a}^+(\omega_2 + \omega_1 - \omega) \hat{a}(\omega_2) \rangle \end{aligned} \quad (\text{A3})$$

everywhere besides $\omega_1 = \omega_2 = \omega$, when arguments of operators on the right part of Eq. (A1) are the same. The field in the FPI is finite so it is reasonable to assume that the $\langle \hat{a}_{\text{in}}^+(\omega) \hat{a}^+(\omega) \hat{a}(\omega) \hat{a}(\omega) \rangle$ does not diverge at any ω . Then the single point $\omega_1 = \omega_2 = \omega$ gives a negligibly small contribution to the integral in Eq. (A1). Therefore, we can neglect the fourth-order correlation, i.e., the case $\omega_1 = \omega_2 = \omega$

in Eq. (A1), and use the expression (A3) instead of $\langle \hat{a}_{\text{in}}^+(\omega) \hat{a}^+(\omega_2 + \omega_1 - \omega) \hat{a}(\omega_2) \hat{a}(\omega_1) \rangle$.

We rewrite Eq. (A3) with the help of the first relation (A2)

$$\begin{aligned} &\langle \hat{a}_{\text{in}}^+(\omega) \hat{a}(\omega_2) \rangle n(\omega_1) \delta(\omega_2 - \omega) \\ &+ \langle \hat{a}_{\text{in}}^+(\omega) \hat{a}(\omega_1) \rangle n(\omega_2) \delta(\omega_1 - \omega), \end{aligned} \quad (\text{A4})$$

replace $\langle \hat{a}_{\text{in}}^+(\omega) \hat{a}^+(\omega_2 + \omega_1 - \omega) \hat{a}(\omega_2) \hat{a}(\omega_1) \rangle$ by the expression (A4) in Eq. (A1), carry out the integration, and find

$$\langle \hat{a}_{\text{in}}^+(\omega) (\hat{n}\hat{a})_{\omega} \rangle = 2n \langle \hat{a}_{\text{in}}^+(\omega) \hat{a}(\omega) \rangle. \quad (\text{A5})$$

The replacement of $\langle \hat{a}_{\text{in}}^+(\omega) \hat{a}^+(\omega_2 + \omega_1 - \omega) \hat{a}(\omega_2) \hat{a}(\omega_1) \rangle$ by Eq. (A3) is similar to the cluster expansion method [36,37], where the mean of a high-order operator product is approximated employing the binary operator products. The approximation is well known in the classical stochastic theory as a ‘‘cumulant-neglect closure’’ [38,39] when the Gaussian distribution approximates the exact classical distribution, so high-order correlations became products of the second-order correlations. In a difference between the cluster expansion and the cumulant-neglect closure approaches applied in the time domain, we make the expansion (A3) in the frequency domain and use it in the integral (A1). In a difference with the time domain, where $\langle \hat{a}^+(t) \hat{a}(t') \rangle \neq 0$ if $t \neq t'$, relations (A2) tell that $\langle \hat{a}^+(\omega) \hat{a}(\omega') \rangle = 0$ if $\omega \neq \omega'$. So the replacement of $\langle \hat{a}_{\text{in}}^+(\omega) \hat{a}^+(\omega_2 + \omega_1 - \omega) \hat{a}(\omega_2) \hat{a}(\omega_1) \rangle$ by Eq. (A3) in the integral (A1) is a good approximation at the stationary case, when relations (A2) are held.

The result (A5) leads to some explicit expressions. We find $\langle \hat{a}_{\text{in}}^+(\omega) \hat{a}(\omega) \rangle$ deriving from Eq. (5)

$$\langle \hat{a}_{\text{in}}^+(\omega) \hat{a}(\omega) \rangle = \frac{i\delta_1 \langle \hat{a}_{\text{in}}^+(\omega) (\hat{n}\hat{a})_{\omega} \rangle + \sqrt{2\kappa} p_{\text{in}}(\omega)}{i(\delta_0 - \omega) + \kappa}. \quad (\text{A6})$$

Substituting the result (A5) into Eq. (A6) we obtain that

$$\langle \hat{a}_{\text{in}}^+(\omega) \hat{a}(\omega) \rangle = \frac{\sqrt{2\kappa} p_{\text{in}}(\omega)}{i(\delta_n - \omega) + \kappa}, \quad (\text{A7})$$

where $\delta_n = \delta_0 - 2\delta_1 n$. Inserting the result (A7) into Eq. (A5) we arrive to the result (8).

Now we find $\langle (\hat{a}^+\hat{n})_{-\omega} (\hat{n}\hat{a})_{\omega} \rangle$ from the energy conservation law $p_{\text{in}}(\omega) = p_{\text{out}}(\omega)$, where $p_{\text{in}}(\omega) = \langle \hat{a}_{\text{in}}^+(\omega) \hat{a}_{\text{in}}(\omega) \rangle$ ($p_{\text{out}}(\omega) = \langle \hat{a}_{\text{out}}^+(\omega) \hat{a}_{\text{out}}(\omega) \rangle$) is the input (output) field power spectrum. The boundary conditions at the semitransparent mirror of the FPI on Fig. 1 lead to $\hat{a}_{\text{out}} = \sqrt{2\kappa} \hat{a} - \hat{a}_{\text{in}}$ and we obtain that $p_{\text{out}}(\omega)$ is

$$\frac{2\kappa \delta_1^2 \langle (\hat{a}^+\hat{n})_{-\omega} (\hat{n}\hat{a})_{\omega} \rangle + i\sqrt{2\kappa} \delta_1 \{ [\kappa + i(\delta_0 - \omega)] \langle \hat{a}_{\text{in}}^+(\omega) (\hat{n}\hat{a})_{\omega} \rangle - \langle (\hat{a}^+\hat{n})_{-\omega} \hat{a}_{\text{in}}(\omega) \rangle [\kappa - i(\delta_0 - \omega)] \}}{(\delta_0 - \omega)^2 + \kappa^2} + p_{\text{in}}(\omega).$$

The energy conservation law $p_{\text{in}}(\omega) = p_{\text{out}}(\omega)$ requires, therefore,

$$2\kappa \delta_1^2 \langle (\hat{a}^+\hat{n})_{-\omega} (\hat{n}\hat{a})_{\omega} \rangle + i\sqrt{2\kappa} \delta_1 \{ [\kappa + i(\delta_0 - \omega)] \langle \hat{a}_{\text{in}}^+(\omega) (\hat{n}\hat{a})_{\omega} \rangle - \langle (\hat{a}^+\hat{n})_{-\omega} \hat{a}_{\text{in}}(\omega) \rangle [\kappa - i(\delta_0 - \omega)] \} = 0. \quad (\text{A8})$$

Substituting the result (8) and the complex-conjugated one $\langle (\hat{a}^+\hat{n})_{-\omega} \hat{a}_{\text{in}}(\omega) \rangle = \langle \hat{a}_{\text{in}}^+(\omega) (\hat{n}\hat{a})_{\omega} \rangle^*$ to Eq. (A8) we obtain the result (10) and calculate the field (11) and the commutator (16) spectra as explained in the main text.

- [1] R. Wang, S. Sprengel, G. Boehm, M. Muneeb, R. Baets, M.-C. Amann, and G. Roelkens, 2.3 μm range InP-based type-II quantum well Fabry-Perot lasers heterogeneously integrated on a silicon photonic integrated circuit, *Opt. Express* **24**, 21081 (2016).
- [2] Q. Liu, J. M. Ramirez, V. Vakarín, X. L. Roux, J. Frigerio, A. Ballabio, E. T. Simola, C. Alonso-Ramos, D. Benedikovic, D. Bouville, L. Vivien, G. Isella, and D. Marris-Morini, On-chip Bragg grating waveguides and Fabry-Perot resonators for long-wave infrared operation up to 8.4 μm , *Opt. Express* **26**, 34366 (2018).
- [3] E. Pelucchi, G. Fagas, I. Aharonovich, D. Englund, E. Figueroa, Q. Gong, H. Hannes, J. Liu, C.-Y. Lu, N. Matsuda, J.-W. Pan, F. Schreck, F. Sciarrino, C. Silberhorn, J. Wang, and K. D. Jons, The potential and global outlook of integrated photonics for quantum technologies, *Nat. Rev. Phys.* **4**, 194 (2022).
- [4] S. Chou, Subwavelength optical elements (soes) and nanofabrications: A path to integrate optical communication components on a chip, in *The 15th Annual Meeting of the IEEE Lasers and Electro-Optics Society* (IEEE, New York, 2002), Vol. 2, pp. 574–575.
- [5] D. Zhu, L. Shao, M. Yu, R. Cheng, B. Desiatov, C. J. Xin, Y. Hu, J. Holzgrafe, S. Ghosh, A. Shams-Ansari, E. Puma, N. Sinclair, C. Reimer, M. Zhang, and M. Lončar, Integrated photonics on thin-film lithium niobate, *Adv. Opt. Photon.* **13**, 242 (2021).
- [6] A. W. Elshaari, W. Pernice, K. Srinivasan, O. Benson, and V. Zwiller, Hybrid integrated quantum photonic circuits, *Nat. Photon.* **14**, 285 (2020).
- [7] L. Zhou, X. Wang, L. Lu, and J. Chen, Integrated optical delay lines: A review and perspective (invited), *Chin. Opt. Lett.* **16**, 101301 (2018).
- [8] G. E. Keiser, A review of WDM technology and applications, *Opt. Fiber Technol.* **5**, 3 (1999).
- [9] M. Sargent, M. O. Scully, and W. E. Lamb, *Laser Physics* (Addison-Wesley, London, 1974).
- [10] J. Kerckhoff, M. A. Armen, and H. Mabuchi, Remnants of semiclassical bistability in the few-photon regime of cavity QED, *Opt. Express* **19**, 24468 (2011).
- [11] M. Kim, I. Hwang, and Y. Lee, All-optical bistability in photonic crystal resonators based on ingaasp quantum-wells, in *All-optical bistability in photonic crystal resonators based on ingaasp quantum-wells* (IEEE, New York, 2006), pp. 769–770.
- [12] L. A. Lugiato, Optical bistability, *Contemp. Phys.* **24**, 333 (1983).
- [13] G. P. Agrawal and H. J. Carmichael, Optical bistability through nonlinear dispersion and absorption, *Phys. Rev. A* **19**, 2074 (1979).
- [14] F. S. Felber and J. H. Marburger, Theory of nonresonant multistable optical devices, *Appl. Phys. Lett.* **28**, 731 (1976).
- [15] I. Protsenko and L. Lugiato, Noiseless amplification in the optical transistor, *Opt. Commun.* **109**, 304 (1994).
- [16] I. E. Protsenko, L. A. Lugiato, and C. Fabre, Spectral analysis of the degenerate optical parametric oscillator as a noiseless amplifier, *Phys. Rev. A* **50**, 1627 (1994).
- [17] C. M. Bowden, M. Ciftan, and H. R. Robl, *Optical Bistability* (Plenum, New York, 1981), p. 614.
- [18] P. D. Drummond and D. F. Walls, Quantum theory of optical bistability. i. nonlinear polarisability model, *J. Phys. A: Math. Gen.* **13**, 725 (1980).
- [19] S. A. Akhmanov, V. A. Vysloukh, and A. S. Chirkin, *Optics of Femtosecond Laser Pulses* (American Institute of Physics, Melville, NY, 1992), p. 366.
- [20] J.-M. Courty and S. Reynaud, Generalized linear input-output theory for quantum fluctuations, *Phys. Rev. A* **46**, 2766 (1992).
- [21] M. J. Collett and C. W. Gardiner, Squeezing of intracavity and traveling-wave light fields produced in parametric amplification, *Phys. Rev. A* **30**, 1386 (1984).
- [22] I. Protsenko, P. Domokos, V. Lefèvre-Seguin, J. Hare, J. M. Raimond, and L. Davidovich, Quantum theory of a thresholdless laser, *Phys. Rev. A* **59**, 1667 (1999).
- [23] E. C. André, I. E. Protsenko, A. V. Uskov, J. Mørk, and M. Wubs, On collective Rabi splitting in nanolasers and nano-LEDs, *Opt. Lett.* **44**, 1415 (2019).
- [24] I. E. Protsenko, A. V. Uskov, E. C. André, J. Mørk, and M. Wubs, Quantum langevin approach for superradiant nanolasers, *New J. Phys.* **23**, 063010 (2021).
- [25] I. E. Protsenko and A. V. Uskov, Quantum fluctuations in the small Fabry-Perot interferometer, *Symmetry* **15**, 346 (2023).
- [26] T. Poston and I. Stewart, *Catastrophe Theory and its Applications* (Dover, New York, 1996), p. 491.
- [27] G. A. Korn, *Mathematical Handbook for Scientists and Engineers* (Dover, New York, 2000), p. 1130.
- [28] J. P. Dahl, The Bohr-Heisenberg correspondence principle viewed from phase space, in *100 Years Werner Heisenberg* (John Wiley & Sons, New York, 2002), pp. 201–206.
- [29] L. D. Landau and E. M. Lifshitz, *Mechanics*, 3rd ed., Course of Theoretical Physics Vol. 1 (Butterworth-Heinemann, Oxford, 1976).
- [30] S. A. Akhmanov and S. Y. Nikitin, *Physical Optics* (Clarendon, New York, 1997), p. 488.
- [31] M. S. Scully and M. O. Zubairy, *Quantum Optics* (Cambridge University Press, Cambridge, England, 1997).
- [32] J. Mørk and G. L. Lippi, Rate equation description of quantum noise in nanolasers with few emitters, *Appl. Phys. Lett.* **112**, 141103 (2018).
- [33] Y. Zhang, Y. Zhao, and R. Lv, A review for optical sensors based on photonic crystal cavities, *Sens. Actuator A: Phys.* **233**, 374 (2015).
- [34] W. Horsthemke and R. Lefever, *Noise-Induced Transitions Theory and Applications in Physics, Chemistry, and Biology* (Springer, London, 1984), p. 322.
- [35] E. Mandel and L. Wolf, *Optical Coherence and Quantum Optics* (Cambridge University Press, Cambridge, England, 1995), p. 1166.
- [36] F. Jahnke, C. Gies, M. Aßmann, M. Bayer, H. A. M. Leymann, A. Foerster, J. Wiersig, C. Schneider, M. Kamp, and S. Höfling, Giant photon bunching, superradiant pulse emission and excitation trapping in quantum-dot nanolasers, *Nat. Commun.* **7**, 11540 (2016).
- [37] C. Gies, J. Wiersig, M. Lorke, and F. Jahnke, Semiconductor model for quantum-dot-based microcavity lasers, *Phys. Rev. A* **75**, 013803 (2007).
- [38] W. Wu and Y. Lin, Cumulant-neglect closure for non-linear oscillators under random parametric and external excitations, *Int. J. Non Linear Mech.* **19**, 349 (1984).
- [39] J.-Q. Sun and C. S. Hsu, Cumulant-neglect closure method for nonlinear systems under random excitations, *J. Appl. Mech.* **54**, 649 (1987).